Structure and metamorphism in the Precambrian Cibola Gneiss and Tijeras Greenstone, Bernalillo County, New Mexico

James R. Connolly

1982, pp. 197-202. https://doi.org/10.56577/FFC-33.197

in:

Albuquerque Country II, Wells, S. G.; Grambling, J. A.; Callender, J. F.; [eds.], New Mexico Geological Society 33 rd Annual Fall Field Conference Guidebook, 370 p. https://doi.org/10.56577/FFC-33

This page is intentionally left blank to maintain order of facing pages.

STRUCTURE AND METAMORPHISM IN THE PRECAMBRIAN CIBOLA GNEISS AND TIJERAS GREENSTONE, BERNALILLO COUNTY, NEW MEXICO

JAMES R. CONNOLLY
Department of Geology/Institute of Meteoritics
University of New Mexico
Albuquerque, New Mexico 87131

INTRODUCTION

Tijeras Canyon is located approximately 21 km east of downtown Albuquerque and is traversed by U.S. Highway 66 and Interstate 40 (1-40). The northeast-striking, subvertical Tijeras fault juxtaposes two mid-Proterozoic age metamorphic terranes of contrasting structural style and lithology. The metamorphic and structural history of these terranes was the subject of a master's thesis by the author. This paper summarizes parts of this thesis, and readers interested in complete presentation of the data and conclusions contained here are referred to Connolly (1981).

This work is based on detailed geologic mapping (generalized in fig. 1), examination of over 200 thin sections, meso- and microscopic petrofabric analysis, and electron microprobe and bulk chemical analyses.

TIJERAS GREENSTONE

The Tijeras greenstone underlies the area southeast of the Tijeras fault. It has been subdivided into a narrow, dominantly metasedimentary terrane adjacent to the fault and a dominantly metabasaltic terrane which underlies most of the area (fig. 1). Mineralogy and probable parent-rock types for the greenstone are summarized in Table 1. The metasedimentary terrane includes chlorite phyllite, biotite phyllite, and metaelastic quartzite, with minor calcic-gneiss and lensoid basic metavolcanic rocks. The metavolcanic terrane includes massive hornblende-andesine metabasalts of tholeiitic composition (Table 2), variably chloritic greenstone and greenschist, minor metasediments and several lenses of felsic metavolcanic rock, two of which are large enough to map (fig. 1). With the local exception of metaclastic quartzite and some blastoporphyritic metabasalts, the rocks are all fine grained with individual crystals rarely more than 1 mm across. Relict phenocrysts of augite are common in the distinctive dark-spotted blastoporphyritic metabasalts. All lithologies except the abundant metabasalts are markedly lensoid and can rarely be traced for more than a few hundred meters.

Two lines of evidence indicate prograde metamorphism of the Tijeras greenstone took place at low-pressure amphibolite facies conditions (about 550±50˚C 50°C and 2±1 kb water pressure). Coexisting andesine and hornblende, detected by electron microprobe in metabasalts of tholeiitic composition, suggest temperatures above 500°C (Liou and others, 1974), and chlorite requires temperatures below 600°C. The presence of andalusite, cordierite, muscovite, and biotite in metapelites indicates a low-pressure metamorphic environment at similar temperatures (fig. 2). Many chlorite phyllites contain sericite-quartz ± chlorite "knots" or spots a millimeter or more across whose composition suggests origin during retrograde metamorphism of andalusite and cordierite at greenschist-facies conditions. Retrograde effects are minimal in massive metabasalts and generally occur as local chloritization of hornblende. In rocks containing more than a few percent chlorite, a crenulation cleavage intersecting foliation at a high angle commonly produces a prominent lineation in the field (fig. 3).

Table 1. Rock types, protoliths, and mineralogy of selected samples of the Tijeras greenstone.

Rock Type (Protolith) \ Minerals	Quartz	Biotite	Muscovite	Andalusite	Cordierite	Garnet	Sericite	Chlorite	Epidote	Hornblende	Actinolite	Plagioclase	Orthoclase	Calcite	Opaque	Augite
CHLORITE PHYLLITE (Shale)	X		X				S	S							0	
Biotite Phyllite (Shale)	X	S	X	S	S	0	0								0	
Quartzite (Metaclastic quartzite)	X		0												0	
CHLORITIC GREENSTONE (Tuff or volcaniclastic?)	S		S				S	X	S	0		X			0	
AMPHIBOLITIC GREENSTONE (Tholeiitic basalt)	0							0	S	X	0	X		0	S	
Blastoporphyritic Greenstone (Tholeiitic basalt)	0							0	S	X		X			S	X
Felsic Metavolcanic (Rhyodacite)	X		S				S					X	X		0	
Calcic Gneiss (Calcareous shale?)						S		0	S	X	S	S		0	S	

All CAPITALS = dominant rock type; lower case = subordinate rock type. X = major constituent (>15% of mode); S = subordinate constituent (3% to 15%); and 0 = minor constituent (<3% of mode).

Table 2. Whole-rock analyses of selected samples of the Tijeras greenstone. Samples analyzed by J. W. Husler.

	1	2	3
SiO_2	51.46	48.26	70.86
TiO_2	0.68	0.50	0.21
Al_2O_3	15.80	18.00	13.75
Fe_2O_3	4.23	2.76	3.63
FeO	6.99	7.37	0.96
MnO	0.29	0.15	0.07
MgO	5.81	8.30	0.58
CaO	9.08	8.94	2.96
Na_2O	2.27	3.21	4.05
K_2O	0.67	0.31	0.84
P_2O_5	0.21	0.04	0.06
SrO	0.02	0.03	0.02
H_2O+	2.07	2.28	1.32
H_2O-	0.18	0.13	0.15
Total	99.76	100.29	99.46

1: Amphibolitic greenstone
2: Blastoporphyritic greenstone
3: Felsic metavolcanic

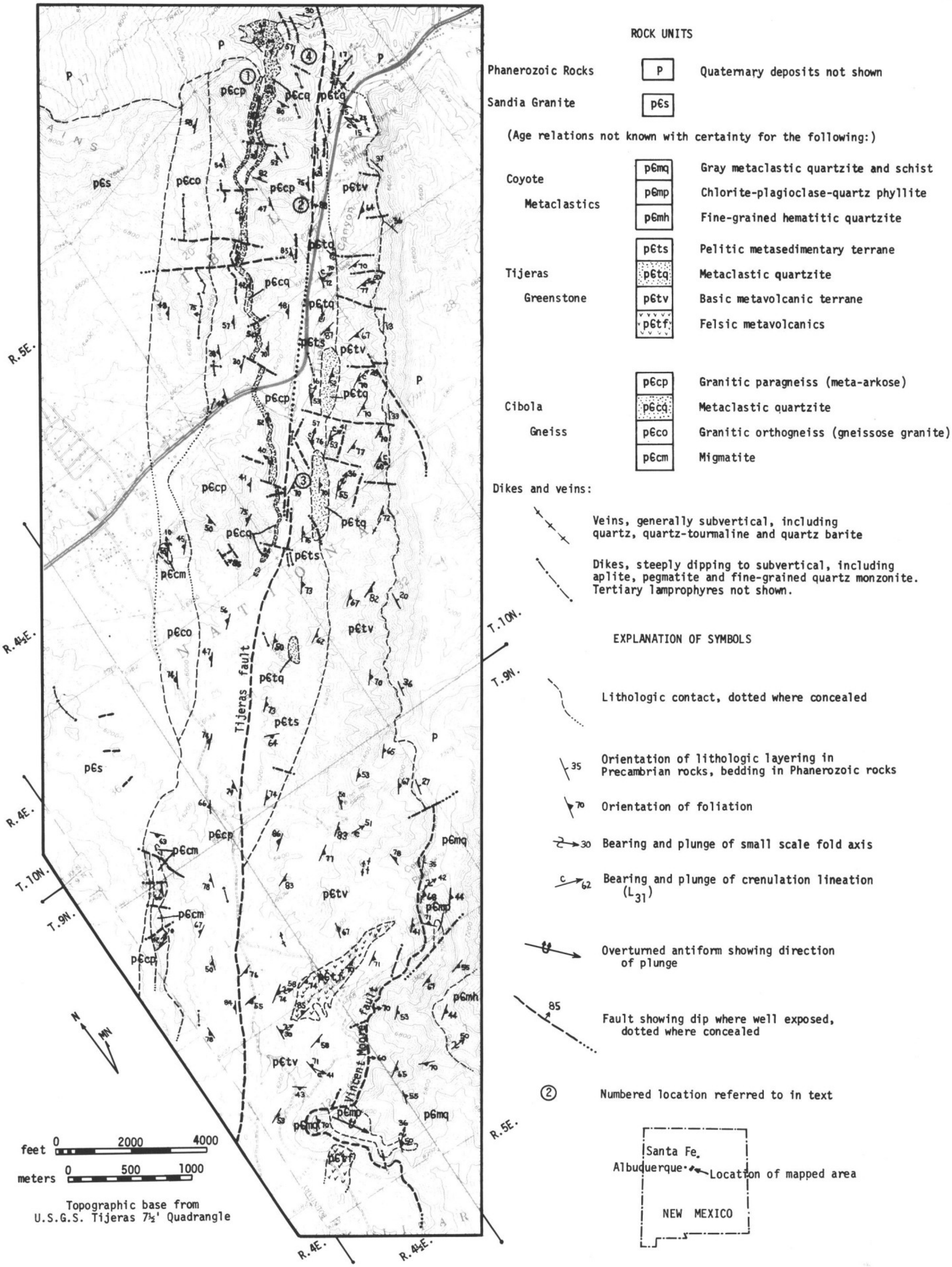

Figure 1. Bedrock geologic map of the Tijeras Canyon area, Bernalillo County, New Mexico (generalized from Connolly, 1981).

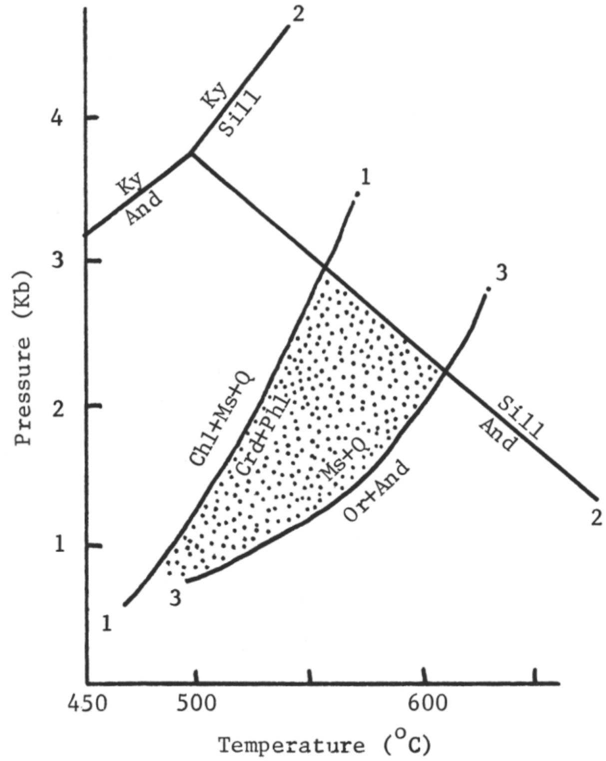

1: Mg-chlorite + muscovite + quartz = Mg-cordierite + phlogopite + H_2O

2: andalusite = kyanite = sillimanite

3: muscovite + quartz = orthoclase + andalusite + H_2O

Figure 2. P-T diagram for Tijeras greenstone. $P_{total} = P_{H_2O}$. Prograde metamorphic field is indicated by stippled area. See Connolly (1981) for references to experimental work on reactions shown.

Throughout the greenstone, lithologic layering (S_0) is approximately parallel to metamorphic foliation (S_1). Foliation morphology varies from phyllitic and locally schistose in metapelites, to a spaced phyllitic cleavage in chloritic greenstone, and to metamorphic mineral banding in plagioclase-amphibole metabasalts. Field relations indicate that S_0 has been transposed parallel to S_1. This evidence includes the presence of parallel lenticular quartzite units at map scale (fig. 1), the lensoid geometry of all rock units, changes of vergence in small-scale fold structures within the same or adjacent outcrops, and the parallelism of S_1 and S_0. Outcrop-scale transposition is characteristic of tectonite terranes which have undergone tight to isoclinal folding at large scale (Turner and Weiss, 1963; R. J. Holcombe, personal commun., 1981).

An S_1-pole diagram of 383 measured foliations in the Tijeras greenstone (fig. 4) shows a tight girdle clustered about a southeast-plunging axis indicating refolding of S_1 about a southeast-plunging (F_2) fold axis. These F_2 folds may be seen in outcrop (fig. 5), hand sample (fig. 6), and in thin section. Prograde metamorphic minerals (chiefly andalusite and cordierite) are locally folded but not significantly altered suggesting F_2 folding occurred at prograde metamorphic conditions. S_2 is poorly defined as the axial planes of small-scale F_2 folds, and S_2 cleavage development is minimal. In general, S_1 and S_2 both dip southeast and lie within 20° of each other. The crenulation cleavage (S_3) developed locally during retrograde metamorphism is variable in orientation but commonly intersects S_1 at angle of more than 45°.

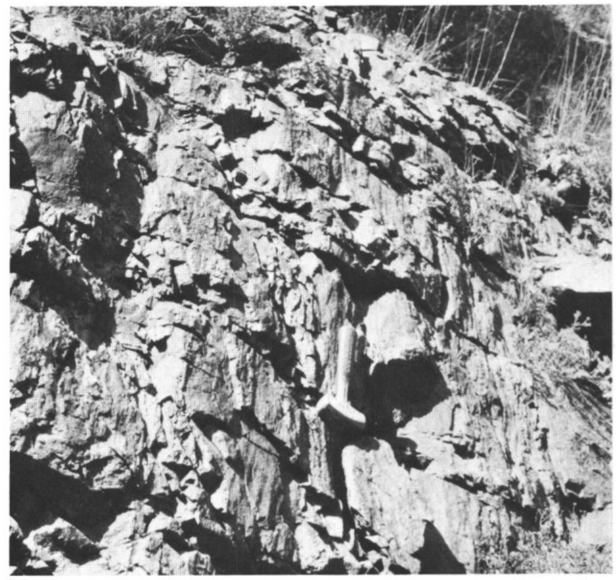

Figure 3. Crenulation cleavage-foliation intersection lineation (L_{31}) in Tijeras greenstone. Hammer head points down-plunge of lineation; plunge is moderate to the southeast.

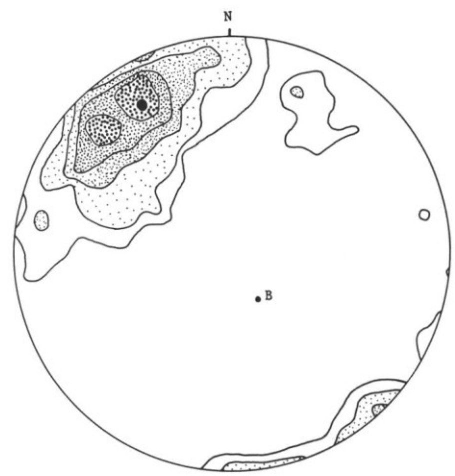

Figure 4. S_1-pole diagram of measured foliation orientation in Tijeras greenstone. 383 data points, contours at 1, 2, 4, 6, and 10 percent per 1 percent area. B is inferred F_2-fold axis.

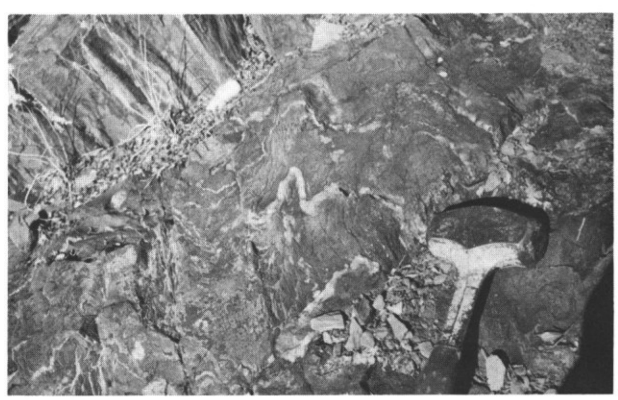

Figure 5. F_2 folds of foliation and quartz-epidote veins in Tijeras greenstone metavolcanics.

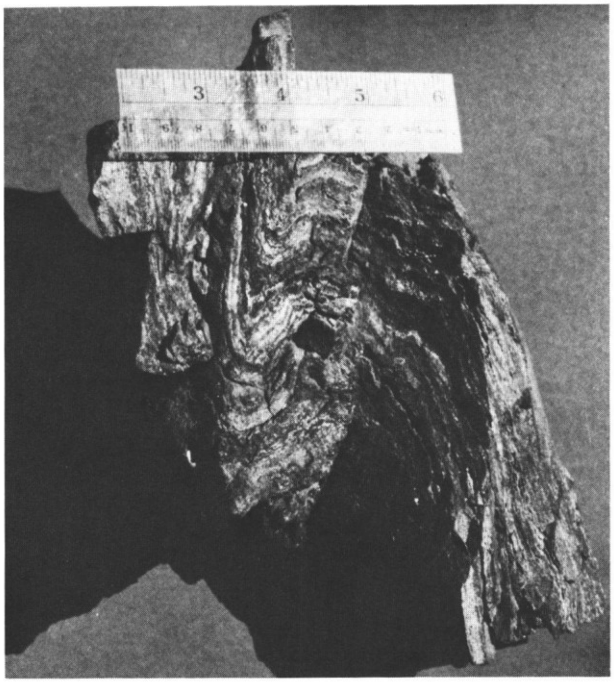

Figure 6. F_2 fold of foliation in amphibolitic greenstone. Scale in inches and centimeters.

The structural data do not allow a reconstruction of stratigraphic relations in the Tijeras greenstone because F_2 folding has drastically modified the original F_1 geometry. The net result is that sections measured perpendicular to lithologic layering (S_0) and foliation (S_1) do not yield stratigraphic information, and that structural relations between F_2 structures and S_0—S_1 likewise cannot be used to develop a stratigraphy.

In summary, the Tijeras greenstone was folded isoclinally and refolded tightly about east-southeast plunging axes at amphibolite-facies conditions, resulting in parallelism of S_0 and S_1 and intersection of S_1 and S_2 at a low angle. Local, retrograde greenschist-facies metamorphism was accompanied by a crenulation cleavage developed at a high angle to S_1.

CIBOLA GNEISS

The Cibola gneiss underlies the area northwest of the Tijeras fault and southeast of the intrusive contact with Sandia granite (fig. 1). Mineralogy and probable protoliths for rocks included in the Cibola gneiss are summarized in Table 3. Meta-arkose dominates the paragneiss portions of the terrane. Fabric varies from weakly foliated to strongly gneissose, and grain size varies from fine to very coarse. Rocks containing more than 10 percent mica tend to be schistose. Within the paragneiss is a resistant ridge of laminated to massive gray quartzite which encloses numerous thin lenses of andalusite-rich schist. Coarsely crystalline, variably gneissose quartz monzonite dominates the orthogneiss portion of the terrane, and two areas of sillimanite-bearing migmatite (injection gneiss and schist) are present close to the granite contact. Minor rock types include thin amphibolite lenses, foliated and non-foliated aplite, and simple pegmatite dikes. Microcline megacrysts up to a few centimeters across are present in Sandia granite and Cibola gneiss and tend to decrease in both size and abundance away from the granite contact. Secondary porphyroblastic muscovite and sercite are developed outside the megacryst-rich zone.

The only reliable indicators of metamorphic grade present in the Cibola gneiss are the aluminum silicates andalusite and sillimanite. Andalusite is abundant in schistose lenses in the quartzite and its ori

Table 3. Rock types, protoliths, and mineralogy of selected samples of the Cibola gneiss.

Rock Type (Protolith) \ Minerals	Quartz	Plagioclase	Orthoclase	Microcline	Biotite	Muscovite	Andalusite	Sillimanite	Opaque	Hornblende
GRANITIC PARAGNEISS (Meta-arkose)	X	S	X	S	S	S			0	
Quartzite (Metaclastic Quartzite)	X						S	0	0	
GRANITIC ORTHOGNEISS (Quartz Monzonite)	X	S	S	X	S	0			0	
Amphibolite (Basalt or Tuff?)	0	X							0	X
Migmatite (Shale?)	X	S			X	S	0	S	0	
Aplite	X	X	X	X		0				
Pegmatite	X	X	X		0	S				

All CAPITALS = dominant rock type; lower case = subordinate rock type. X = major constituent (>15% of mode); S = subordinate constituent (3% to 15%); and 0 = minor constituent (<3% of mode).

entation parallel to metamorphic foliation suggests that it crystallized syntectonically. Sillimanite is abundant in migmatite adjacent to Sandia granite and locally developed within otherwise massive quartzite; orientation is largely random and suggests origin during post-tectonic thermal metamorphism. Previous workers (Kelley and Northrop, 1975; have used the presence of microcline porphyroblasts to infer upper amphibolite facies conditions for the Cibola gneiss. Three lines of evidence support a metasomatic origin for these porphyroblasts. Firsi is the decrease in size and abundance away from the granite contact. Second is the tendency for porphyroblasts to grow in granite, gneiss, and magmatic inclusions in granite (fig. 7) with apparent disregard foi host-rock composition. Third, in thin sections the porphyroblasts clearly replace earlier phases and overgrow gneissose fabrics. Muscovite i5 commonly replaced, and yet, aluminum silicates are notably absent suggesting crystallization by a metasomatic reaction similar to:

$$\text{muscovite} + \text{quartz} + K^* = \text{K-feldspar} + H' .$$

Figure 7. Metasomatic microcline porphyroblasts (m) grown in inclusion (outlined) and Sandia granite host rock. Scale is 15 cm long.

Figure 8. Isolated fold hinges in quartzite of Cibola gneiss. View is to northeast in thickened area within hinge region of map-scale fold (loc. 1, fig. 1). Divisions on staff are 10 cm intervals.

Figure 9. Transposed magnetite-rich bands in quartzite of Cibola gneiss on northwest limb of map-scale overturned antiform (fig. 1).

Figure 10. Small-scale isoclinal F_1 folds in hinge region of map-scale antiform in quartzite of Cibola gneiss. View is to northeast.

This reaction may occur over a range of temperature between 300°C and 600°C and is strongly dependent on the activities of K and 1-1+ (Montoya and Hemley, 1975). High K+ activity favors the forward reaction which releases 1-1+ and may account for the outer halo of sericitic alteration seen in the Cibola gneiss.

Little may be said with certainty about the metamorphic environment in the Cibola gneiss except that synkinematic metamorphism probably occurred within the stability field of andalusite at relatively low pressure, and that late thermal metamorphism associated with granitic intrusion locally elevated temperatures into the stability field of sillimanite. Gneissose fabrics suggest amphibolite facies during synkinematic metamorphism, and incipient melting in migmatites suggest temperatures near the granite contact between 650°C and 750°C (Winkler, 1976).

Most structural data for Cibola gneiss come from the quartzite unit. Foliation (S,) in the quartzite is defined by the orientation of flattened quartz grains in massive quartzite and schistosity in andalusite-mica lenses. Layering (S_0) is defined by color banding in quartzite, dark magnetite-rich bands, and quartzite-schist contacts. S„ and S, are invariably sub-parallel or parallel implying isoclinal folding and transposition of S. Transposition is also indicated by isolated fold hinges (fig. 8), discontinuous bands of magnetite (fig. 9), and outcrop-scale isoclinal folding (fig. 10). On the large-scale, isoclinal (F,) folding of the quartzite unit (and thus of the enclosing paragneiss) is evidenced by structural closure (fig. 11) indicating gentle northeast plunge and extensive thickening in the hinge region in the northern part of the mapped area (loc. 1, fig. 1). F, in the quartzite is defined by small-scale tight folds of S_1 whose axes tend to plunge down the dip of S_1 to the northwest so that S, lies almost 90° from S_1. No large-scale F, folds occur in the study area. F, is defined by minor, locally developed open flexures of S, about northwest-plunging axes.

In summary, the Cibola gneiss was folded isoclinally about gently northeast-plunging fold axes, probably at low-pressure amphibolite facies metamorphic conditions. Tight refolding followed about northwest-plunging axes at a high angle to the first folding. This resulted in parallelism of S_0 and S_1 and intersection of S_1 and S, at close to 90°. A late, post-kinematic thermal metamorphic-metasomatic event related to Sandia granite intrusion resulted in local sillimanite crystallization and a potassic-sericitic alteration halo overprinted on the granite-gneiss boundary which produced a gradational granite-gneiss contact.

TIJERAS FAULT

The Tijeras fault separates the Cibola gneiss and Tijeras greenstone everywhere within the mapped area (fig. 1). The fault strikes N35°E to N45°E and is approximately vertical; it is part of a major northeast-striking system of faults and intrusive centers which has a complex history of activity spanning Precambrian through Quaternary time (Lisenbee and others, 1979).

Exposures along roadcuts on 1-40 (loc. 2, fig. 1) juxtapose greenstone and colluvium and indicate some Quaternary dip-slip movement has occurred at least locally (see road-log segment I-A, this guidebook).

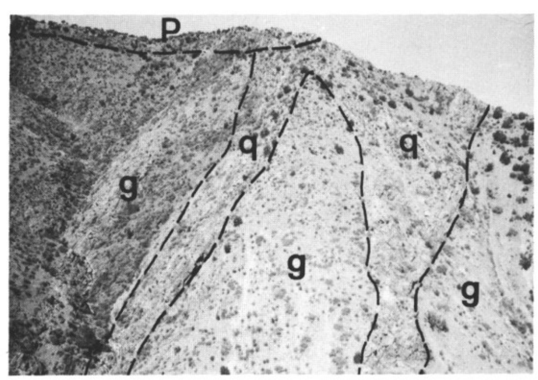

Figure 11. Structural closure in isoclinally folded quartzite (q) in Cibola gneiss (g), with overlapping upper Paleozoic strata (P). View is northeast toward Location 1 on Figure 1.

South of 1-40 (loc. 3, fig. 1), numerous unmetamorphosed quartz veins, simple pegmatites, and fine-grained granitic dikes intrude greenstone adjacent to the Tijeras fault. The dikes are discordant to foliation, strike slightly more northerly than the fault, are subvertical or dip steeply southeast, and are arranged in a right-stepping en-echelon pattern relative to the fault. The localization of these features near the fault suggests intrusion and fault activity were contemporaneous, and the en-echelon arrangement suggests left slip. Radiometric ages of granitic plutons in central New Mexico fall in the general range of 1.4 to 1.7 b.y. (Condie, 1981; Brookins, and Brookins and Majumdar, this guidebook), and Tijeras fault activity is probably at least as old as plutonism.

An area within the Cibola gneiss near the northeastern edge of the mapped area (loc. 4, fig. 1) shows a well developed fracture and minor fault pattern dominated by northwest-striking, right-lateral shears offsetting north-striking pinnate quartz veins (fig. 12a). When considered in conjunction with the Tijeras fault and granitic dikes in the greenstone, these structures suggest an origin for this part of the Tijeras fault during approximately north-south compression in Proterozoic time (fig. 12b).

Foliation in the Tijeras greenstone is sharply discordant to the strike of the fault at most locations examined, while foliation in the Cibola gneiss is commonly discordant but locally is nearly parallel to the fault strike. No mylonitic rocks are clearly associated with the fault in either of the bounding terranes, although poorly consolidated breccia is present in both.

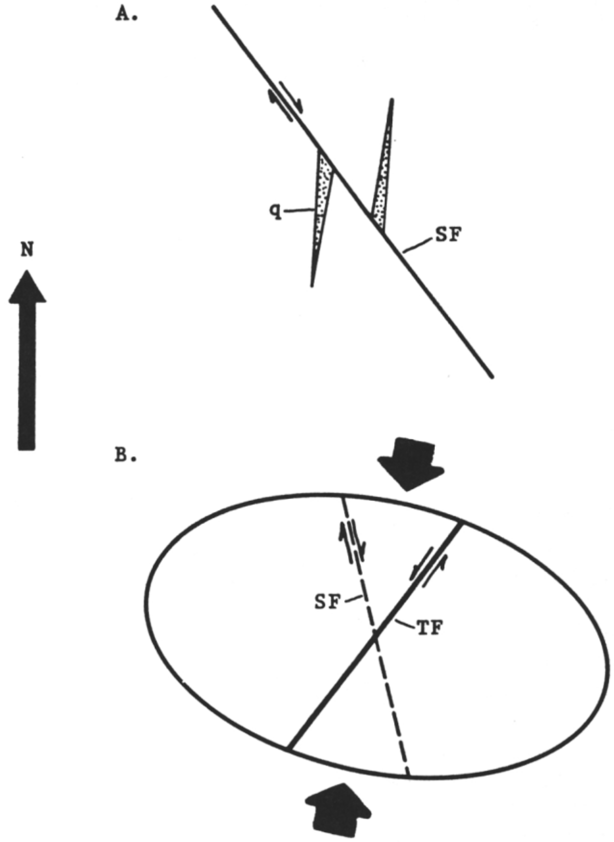

Figure 12. Synoptic structure diagram of Tijeras fault. (a) Plan geometry of shear fractures (SF) and pinnate quartz veins (q) in Cibola gneiss (loc. 4, fig. 1). (b) Generalized strain ellipse during inception of Tijeras fault (TF). See text for discussion.

CONCLUSIONS

The Cibola gneiss and Tijeras greenstone were both isoclinally folded (F_1) syntectonically with low-pressure amphibolite facies metamorphism. The geothermal gradient was at least 40°C per km based on aluminum silicate equilibrium. For the greenstone, additional mineralogic constraints suggest gradients of 70°C per km or more.

The greenstone was refolded tightly about F_2 axes approximately parallel to F_1 axes, while gneiss was refolded tightly about F_2 axes at a high angle to F_1.

Sandia granite produced a sillimanite grade contact aureole surrounded by a potassic-sericitic alteration halo in Cibola gneiss resulting in a gradational gneiss-granite contact. Although some pegmatitic and granitic dikes intrude Tijeras greenstone, no high-temperature thermal effects are noted, and the latest metamorphic event noted is retrograde chlorite-sericite greenschist facies developed in crenulated phyllites.

Granitic-pegmatitic dike geometry relative to the Tijeras fault suggests left-slip syntectonic with granitic intrusion (-1.5 b.y.). The contrasts in lithology, structural geometry, and metamorphic history suggest at least several kilometers of left-slip on the Tijeras fault.

REFERENCES

Condie, K. C., 1981, Precambrian rocks of the southwestern United States and adjacent areas of Mexico: New Mexico Bureau of Mines and Mineral Resources Resource Map 13.

Connolly, J. R., 1981, Geology of the Precambrian rocks of Tijeras Canyon, Bernalillo County, New Mexico (M.S. thesis): University of New Mexico, Albuquerque, 147 p.

Kelley, V. C. and Northrop, S.A., 1975, Geology of the Sandia Mountains and vicinity, New Mexico: New Mexico Bureau of Mines and Mineral Resources Memoir 29, 136 p.

Liou, J. G., Kuniyoshi, S., and Ito, K., 1974, Experimental studies of the phase relations between greenschist and amphibolite in a basaltic system: American Journal of Science, v. 274, p. 613-632.

Lisenbee, A. L., Woodward, L. A., and Connolly, J. R., 1979, Tijeras-Canoncito fault system—a major zone- of recurrent movement in north-central New Mexico: New Mexico Geological Society Guidebook 30, p. 89-99.

Montoya, J. W. and Hemley, J. J., 1975, Activity relations and stabilities in alkali feldspar and mica alteration reactions: Economic Geology, v. 70, p. 577-583.

Turner, F. J. and Weiss, L. E., 1963, Structural analysis of metamorphic tectonites: McGraw Hill, New York, 545 p.

Winkler, H. G. F., 1976, Petrogenesis of metamorphic rocks Springer-Verlag, New York, 4th edition, 334 p.